# Improving High Dynamic Range Image Based Light Measurement

Hankun Li
Civil, Environmental and Architectural Engineering, School of Engineering
University of Kansas
Lawrence, Kansas, USA
hankunli@ku.edu

Hongyi Cai
Civil, Environmental and Architectural Engineering, School of Engineering
University of Kansas
Lawrence, Kansas, USA
hycai@ku.edu

Guanghui Wang
Electrical Engineering and Computer Science, School of Engineering
University of Kansas
Lawrence, Kansas, USA
ghwang@ku.edu

***Abstract*—This study proposes a fast-high dynamic range imaging technique for light measurement to short the long capturing time of current camera-aided computational photography widely used in lighting practice. In comparison with conventional meter measurement, High-Dynamic-Range Imaging (HDRI)-assisted lighting measurement is a remote, efficient, and affordable method, yet time-consuming. This study proposes to increase film speed (ISO) to speed up taking a sequence of low dynamic range images. Since the increased camera's film speed will introduce more image noise, the possible error rate of the proposed method was evaluated by applying Gaussian noise estimation and impulsive noise detection on the image with different film speeds. In addition, a new per-pixel calculation process was developed to retrieve the illuminance of a target scene with selected areas of interest, which can be applied to assist human-centric lighting tasks. Extensive comparative experiments have been conducted to verify the accuracy and efficiency of the proposed method.**

***Keywords— High dynamic range image, light measurement, luminance, illuminance***

## I. INTRODUCTION

The purpose of this study is to improve the performance of the current high dynamic range image (HDRI) based light measurement. Light measurement is important in both scientific studies and design projects. Conventional meter measurements, which include point-by-point luminance measurement, are sometimes very tedious and low efficient. Illuminance measurement and spectrum measurement are often conducted separately (Cai, 2012). For example, conducting a meter measurement of light for a scene with point-by-point luminance measurement takes lots of time and labors. The meter measured illuminance can only reflect the general light level of the scenario, which probably hard to understand for non-lighting professionals without a visualized output. Another limitation of conventional meter measurement is that the results may not reflect real-time lighting conditions, especially for measurement conducted in some fast light-changing scenarios (e.g., daylit space).

Camera aided light measurement (HDRI based) can capture the full range of luminance and color values of the target scene and store them by pixels, which can be recovered as a lighting information map of the scene later (Ward G. et al., 2010). The HDRI based light measurement has been introduced to lighting professional for more than one decade and become popular recently, as its visualized output have more practical usages and very easy to understand.

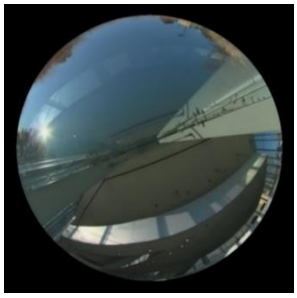

Figure 1 Sun position changing in daylit space

Figure 2 Ghosting effect caused by moving people

The current methods for taking a high dynamic range light probe image need 60 to 150 seconds depends on the dynamic range target scene with fixed film speed: ISO100 (Inanici 2009, Cai & Chung 2011, Pierson & Wienold 2017, Pierson et al. 2020). To maximize the accuracy of the retrieved light information, the ISO is fixed to 100, which is good for taking HDRI in a static scenario. However, the measurement accuracy of the light changing environment (e.g., daylit space in Figure 1) could be greatly reduced. The most ghosting effect produced by moving people and/or objects in the target scene can be eliminated by ghosting removal algorithm (Silk & Lang, 2012). Some ghosting effects in the HDR image without good contrast to its background are hard to detect and remove, as shown in the marked portion of Figure 2.

The illuminance of the measured scenario can be calculated by evalglare (Wienold 2006, Pierson et al. 2020), which is widely used by lighting researchers. Two limitations of the radiance based evalglare were found in this study. First, it can

only output a single illuminance of the target scene without a visualized distribution map. Second, the running time of evalglare is fast only if the HDR probe image is cropped and resized to 800 by 800 pixels (Pierson et al. 2020), otherwise, the speed could be slow with its original resolution. Another practical problem is that the camera control software used in those existing methods for taking sequenced low dynamic range images has some limitations. Cai used DSLR Control Pro for camera control (Cai, 2011&2013) and Pierson used qDslrDashboard (Pierson et al. 2020) for taking those low dynamic range images. DSLR Control Pro only allows a maximum of 15 shots in auto-bracket mode, which means any extra low dynamic range images exceed fifteen limits could only be taken manually.

This study aims to improve HDRi based lighting measurement in two aspects. First, optimizing time-delay errors by shortening the time for taking a high dynamic range image for light measurement. The negative impact of using higher film speed (ISO) was evaluated with the level of Gaussian noise and impulsive (salt-and-pepper) noise of images taken with different film speeds. Four experimental light measurements were conducted for comparing luminance and illuminance measurement accuracy and total time consumption.

Figure 3 A sample HDR image for light measurement of a laboratory

In addition, an illuminance calculation method was developed based on the hemispherical surface integral with the specified camera lens projection function. As shown in Figure 3, users may be interested in how much light could be perceived from the window (marked in red) and overhead luminaries (marked in blue).

***Significant results of this study***

The experimental results demonstrate that the ISO increasing method proposed in this study could reduce the total exposure time from 85 seconds to 19 seconds, while still achieving the best luminance error rate of 2.5%, an average luminance error rate of 4.5%, and an illuminance error rate of 4.15% compared with meter measurement. The newly developed per-pixel illuminance calculation program is 2 times faster and 7 times faster in fast mode than the illuminance calculation of evalglare on the same HDR image with resolution of 5184 by 3456 pixels.

## II. Related Works

The contrast ratio of luminance in the most real-world scenarios exceeds the capability of digital cameras for capturing the full dynamic range of a scene in a single shot. Using standard digital single-lens reflex (DSLR) camera fitted with the proper lens, one can create a High Dynamic Range (HDR) image from multiple Low Dynamic Range (LDR) photographs with different exposure values (Mann, Picard 1995). To do so, one has to capture multiple LDR images covering the full luminance details of the target scene and linearize the LDR images with the inverse function of the camera response function (CRF), then average them with specified weighting function and eventually fuse them into a single HDR image (Greg 2010). However, one inherent shortage for most digital camera sensors is the limited dynamic range or contrast ratio of each capture, since not all pixels record the correct light information because of improper over- or under-exposures. By taking multiple exposures of a target scenario, each exposure contains some properly exposed pixels and other pixels might be over-exposed and/or under-exposed. The correct lighting data map of the target scene can be retrieved with each pixel in correspondence to one or more correct exposures (Greg 2010).

The standard exposure value could be calculated with three variables of a digital camera: aperture size, shutter speed, and film speed (ISO). The basic function with film speed (ISO 100) is a base-2 logarithmic scale (Ray, 2000). With different ISO value, the conversion of exposure value can be expressed in equation 1:

$$EV_{100} = log_2 \frac{N^2}{t}\frac{100}{S} \quad (1)$$

EV100 is the standard exposure values, N is for aperture size of the camera lens, t is the shutter speed in seconds and S is the ISO value set on the digital camera.

The aperture size affects the depth of field (another factor is focal length). Smaller aperture stops (bigger f-number) produces a longer depth of field, which allows objects at a further range of distance can still be focused and clearly captured by the image sensor. The aperture stops are also related to optical aberrations. If the aperture size is too large (smaller f-number), the image may have distortion (elite-cameras.com, 2006). The optical vignetting effect is sensitive to the lens aperture, which is an unwanted effect in the image-based lighting measurement. Using larger aperture will cause more vignetting effect, as the intensity of light reaching the image sensor falls off toward the edges of the picture, especially for off-axis viewing directions (Catrysse, Liu and Gamal, 2000). The vignetting correction curve of the fisheye lens can be derived by panoramic rotation that is commonly used (Inachi 2006, Cai & Chung 2011).

## III. Methodology

To realize the proposed technology and apply it for conducting experiments in this study, a camera control with the desired function was developed based on Python gphoto2 library (gphoto.org). The customized impulsive noise detection was developed with unsharp masking and canny edge detector and

the Gaussian noise detection was conducted by using the weak texture patch method (Liu et al. 2012). Both noise detections were implemented for quantifying images noise of image taken with different ISO. The proposed illuminance calculation from the High Dynamic Range probe image is derived from the hemisphere surface integral with input camera lens projection function. This newly developed program allows using different fisheye lens projection input and enables the output illuminance contribution with a region of interest selection, which could be useful for human-centric tasks like figuring out how much light emitted from artificial light sources eventually come to human eyes (Cai 2020). Also, an output illuminance distribution map can help non-lighting professionals to better understand the light distribution of a scenario.

### *A. Developed an auto-bracket program for implementing the dedicated exposure sequences.*

In contrast to DSLR control software only allowing users to implement an auto-bracket with only shutter speed sequenced and limit 15 maximum sequences, the newly developed auto-bracket program allows users to modify the camera value setting for every single shot with unlimited total sequences. The improved auto-bracket program was developed in Python with gphoto2 (running on the Linux system). Raspberry Pi 3B+ is used as the portable camera control for the running program in this study.

The improved auto-bracket program also enables a better auto-bracket strategy: using high ISO value for higher exposure level sequences to reduce time consumption and using low ISO value for lower exposure level sequences to minimize noise and maintain image quality. For example, using ISO 6400 with a shutter speed of 0.5 seconds could reach the same exposure level of ISO 100 with a shutter speed of 30 seconds but reduce the time consumption from 30 seconds to 0.5 seconds. There are two main reasons to propose this strategy: first, mixing high ISO LDR images with low ISO LDR images could greatly reduce total time consumption and keep the same level of luminance accuracy and minimize loss of image quality compare to all LDR images captured with low ISO value. The second reason is that hardware action needs time for processing. Since the signal communication between the control device and the camera take approximatly 0.3 seconds, increasing ISO value for these lower exposure value images could not reduce time consumption but loss high level of image quality.

### *B. Impulsive noise of images with different ISO*

Using higher ISO value on camera increases the image noise level, including Gaussian noise and impulsive noise. Both types of image noise are random noise, as the impulsive distribution follows probability Fat-tailed distribution that exhibited a large skew pattern, and the gaussian noise follows the normal distribution. An image containing impulsive noise has dark pixels in bright regions and bright pixels in dark regions, which is also called “salt and pepper” noise. This type of noise can be caused by analog-to-digital converter errors, bit errors in transmission, or sensor temperature rising, etc. (Bovik 2005).

Figure 4 Color checker image taken with ISO 100

This study proposed impulsive noise evaluation on color checker images (Figure 4) with a different camera ISO value, which could be a general guide for taking HDR images with a balance between speed and image quality. The evaluation program was developed based on salt-and-pepper noise detection with gaussian blur and unsharp masking.

Table 1 Impulsive noise of color checker image (ISO 100 to 6400)

| ISO | **100** | **200** | **400** | **800** |
|---|---|---|---|---|
| Noise rate | 0.0015% | 0.0015% | 0.0015% | 0.0017% |
| ISO | **1600** | **3200** | **6400** | |
| Noise rate | 0.0024% | 0.0035% | 0.0210% | |

Table 1 is the results of impulsive noise detected on color checker images taken with ISO from 100 to 6400. The percentage in Table 1 is the ratio of pixel detected as impulsive noise to the total pixel. The noise rate color checker image with ISO lower than 400 are the same, which can be considered as a defective pixel on the image sensor. The impulsive noise on the image with ISO between 800 to 1600 is still acceptable (lower than 0.01%). However, the impulsive noise rate of ISO 6400 image is 6 times of ISO 3200, which is the worst case in this study.

Table 2 Color error of color checker image with ISO from 200 to 6400

| ISO | | **200** | **400** | **800** | **1600** | **3200** | **6400** |
|---|---|---|---|---|---|---|---|
| **Relative Error** | R | 0.087% | 0.086% | 0.084% | 0.195% | 0.210% | 0.301% |
| | G | 0.073% | 0.075% | 0.101% | 0.188% | 0.220% | 0.263% |
| | B | 0.076% | 0.091% | 0.153% | 0.219% | 0.220% | 0.262% |

Table 2 shows the color noise error of color checker image with ISO from 200 to 6400 of each color channel. Using the color checker image with ISO 100 as the baseline of evaluation, the percentage value in Table 2 indicates the ratio of pixel errors in each color channel compared to the baseline error rate.

### *C. Gaussian noise of image with different ISO*

Gaussian noise is another type of random noise that follows the normal distribution. Therefore, the level of Gaussian noise of image can be quantified by evaluating the variance of pixel intensity of RGB channel on the weak patches extracted from the uniform background of the image. The algorithm for gaussian noise estimation is to calculate the sigma value of the normal distribution from the sample patch (Liu, Tanaka, Okutomi 2012).

Table 3 The σ of gaussian noise of HDR image with different ISO

| | ISO | 200 | 400 | 800 | 1600 | 3200 | 6400 |
|---|---|---|---|---|---|---|---|
| σ | Patch1 | ~ 0 | ~ 0 | ~ 0 | 0.0198 | 0.0742 | 0.1215 |
| | Patch2 | ~ 0 | ~ 0 | ~ 0 | 0.0212 | 0.0778 | 0.1227 |
| | Patch3 | ~ 0 | ~ 0 | ~ 0 | 0.0183 | 0.0733 | 0.1118 |

As shown in Table 3, the evaluated σ value of normal distribution for demonstrating the Gaussian noise of sample patches (marked yellow in Figure 5) from HDR images with ISO from 200 to 6400.

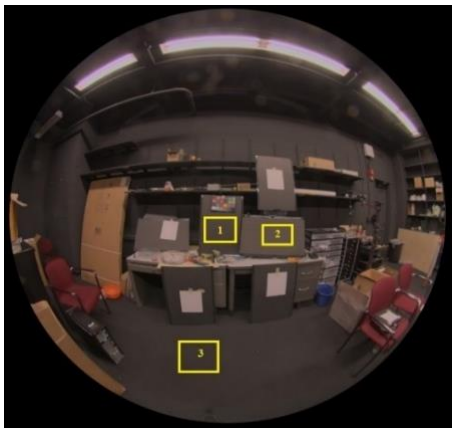


Figure 5 Sampled patches for evaluating gaussian noise

### D. *Calculating the illuminance from Radiance High Dynamic Range image with selected region of interest.*

This study developed an algorithm based on the surface integral of the hemisphere function for calculating illuminance from radiance High Dynamic Range images (.hdr). Proposed per-pixel calculation MATLAB program have a higher running speed than current illuminance calculation in evalglare. As the illuminance was calculated from integration, the proposed calculation is less sensitive to image resolution change and lower error can be expected. The kernel function is:

$$E = \sum_{d=0}^{r} \sum L_{i_d} \int_{\theta_i'}^{\theta_i''} \frac{2\pi(cos\theta_i' - \cos\theta_i'')}{(\theta_i'' - \theta_i')\sum i_d} \; cos\theta \; d\theta \qquad (2)$$

E is the illuminance (lux) of the target scene measured at the camera lens. d is the distance of the pixel center to image center on the image sensor and the r is the maximum distance, which is the 'radius' of the circular HDR image on the image sensor. $\theta_i'$ is the top altitude angle of the pixel I and $\theta_i''$ is the bottom altitude angle of pixel i, they can be considered as 'start' altitude angle and 'end' altitude angle of integration of each pixel. $L_i$is the luminance of pixel i.

The fisheye projection function of the circular image is used for assigning the altitude of each pixel. The camera lens used in this study is an equi-solid angle projection fisheye lens. As the projection function shown below:

$$\theta = 2\arcsin\left(\frac{d}{2f}\right) \qquad (3)$$

d is the distance from the center of pixel i to the image center. f is the focal length of the fisheye lens and $\theta$ is the altitude angle of the pixel. The illuminance of the scene can be calculated as the sum of per-pixel cosine corrected illuminance that could be considered as a contribution of illuminance from every direction of the scene (Equation 4).

$$E = \sum_{i=1}^{n} \int_{\theta_i'}^{\theta_i''} L_i \, d\Omega \, cos\theta d\theta \qquad (4)$$

$L_i$ is the luminance of a pixel on the circular image, which represents the incident luminance from that direction on the scene and the $d\Omega$ is the solid angle of the apparent area of that pixel i.

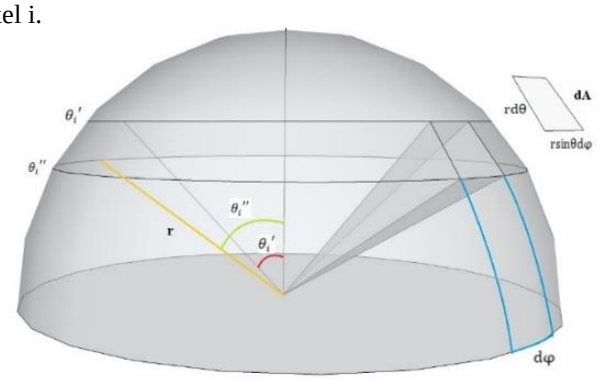


Figure 6 visualized illuminance calculation

Since the illuminance measured here is the illuminance perpendicular to the measurement plane (image plane), cosine correction is required to apply on every pixel to calculate the vertical component of illuminance (Figure 6).

In Equation 5, $d\Omega$ is calculated as apparent area dA divided by the square of radius r.

$$d\Omega = \frac{dA}{r^2} \qquad (5)$$

As shown in Figure 6, the small area dA could be considered as a small rectangular area with the calculation of equation 6.

$$dA = (\mathrm{rsin\theta d\varphi})(\mathrm{rd\theta}) \qquad (6)$$

Equation 7 shows the calculation of small area dA in the digital image. dA is calculated as the total area between $\theta_i'$ and $\theta_i''$ on the sphere divided by the total number of pixels with altitude angle between $\theta_i'$ and $\theta_i''$ ($\sum i_d$). The total surface area between $\theta_i'$ and $\theta_i''$is calculated by area of sphere cap (Gibson & Scheraga 1987). Combining Equations 4, 5, and 7, the illuminance calculation function (equation 2) is proven.

$$dA = \frac{2\pi r^2(cos\theta_i' - \cos\theta_i'')}{(\theta_i'' - \theta_i')\sum i_d} \qquad (7)$$

As the illuminance of the target scene is calculated from per-pixel contribution (Figure 7), the distribution of illuminance could be recovered from the output.

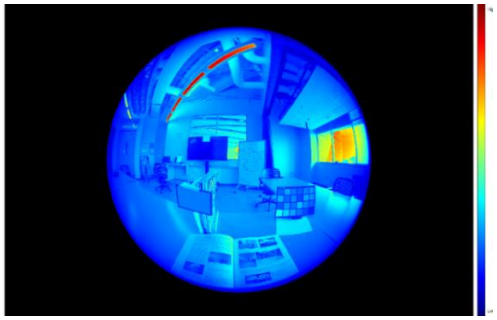

Figure 7 The gradient map of perceived light (631 lux)

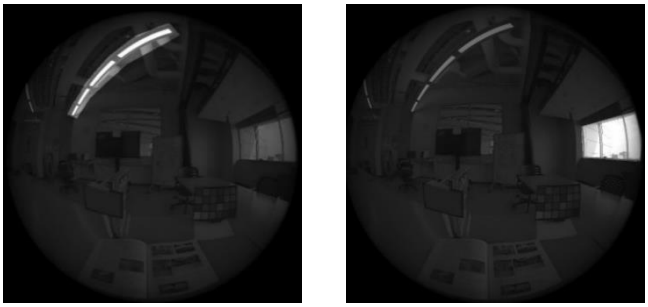

Figure 8 light from interested areas (left: from overhead fluorescent, 167 lux, 26.4% of total; right: from window, 192 lux, 30.4% of total)

Users could easily figure out how much light that human eyes could be perceived from which parts of the scene or from which direction. For example, in Figure 8, 26.4% light of viewpoint coming from overhead fluorescent and 30.4% light coming from the window.

## IV. Experimental Results

This experiment was conducted in the darkroom of the University of Kansas lighting research laboratory, which is well controlled with an interior correlated color temperature of 3350 kelvin.

Table 4 Schedules of LDR images for merging HDR image

| Original | | High Noise | | Combination #1 | | Combination #2 | |
|---|---|---|---|---|---|---|---|
| ISO | Shutter speed | ISO | Shutter speed | ISO | Shutter speed | ISO | Shutter speed |
| 100 | 30s | 6400 | 1/2s | 6400 | 1/2s | 6400 | 1/2s |
| 100 | 15s | 6400 | 1/4s | 3200 | 1/2s | 6400 | 1/4s |
| 100 | 8s | 6400 | 1/8s | 1600 | 1/2s | 6400 | 1/8s |
| 100 | 4s | 6400 | 1/15s | 800 | 1/2s | 6400 | 1/15s |
| 100 | 2s | 6400 | 1/30s | 400 | 1/2s | 6400 | 1/30s |
| 100 | 1s | 6400 | 1/60s | 200 | 1/2s | 6400 | 1/60s |
| 100 | 1/2s | 6400 | 1/125s | 100 | 1/2s | 6400 | 1/125s |
| 100 | 1/4s | 6400 | 1/250s | 100 | 1/4s | 6400 | 1/250s |
| 100 | 1/8s | 6400 | 1/500s | 100 | 1/8s | 100 | 1/8s |
| 100 | 1/15s | 6400 | 1/1000s | 100 | 1/15s | 100 | 1/15s |
| 100 | 1/30s | 6400 | 1/2000s | 100 | 1/30s | 100 | 1/30s |
| 100 | 1/60s | 6400 | 1/4000s | 100 | 1/60s | 100 | 1/60s |
| 100 | 1/125s | 3200 | 1/4000s | 100 | 1/125s | 100 | 1/125s |
| 100 | 1/250s | 1600 | 1/4000s | 100 | 1/250s | 100 | 1/250s |
| 100 | 1/500s | 800 | 1/4000s | 100 | 1/500s | 100 | 1/500s |
| 100 | 1/1000s | 400 | 1/4000s | 100 | 1/1000s | 100 | 1/1000s |
| 100 | 1/2000s | 200 | 1/4000s | 100 | 1/2000s | 100 | 1/2000s |
| 100 | 1/4000s | 100 | 1/4000s | 100 | 1/4000s | 100 | 1/4000s |

Table 4 shows four different LDR images' schedules for taking HDR images with same EV range: original settings (ISO100), high noise settings (Maximize ISO for each exposure), combination 1 (less ISO 6400 images) and combination 2 (more ISO 6400 images). HDR images in this experiment was taken by Canon 550D with SIGMA f-2.8 fisheye lens. The ground truth value of luminance and illuminance were measured by Minolta LS-100 and Minolta CL500A. Accuracy of luminance and illuminance and time consumption were compared between four HDR images taken with different LDR images schedules but with the same EV range.


Figure 9 Reference points of the target scene

Figure 9 is the setup of this experiment with all reference targets marked. These refence targets including four white print paper as well as a 18% gray checker.

Table 5 real time consumption for taking HDR images

| | Original | High noise | Combination #1 | Combination #2 |
|---|---|---|---|---|
| Real Time (secs) | 85 | 16.5 | 18 | 19 |

As shown in Table 5, LDR images with original settings are captured by DSLR control pro software, which takes 85 seconds to finish. The other three HDR images with combined camera film speed are captured by custom developed auto-bracket program running on Raspberry Pi 3B plus.

Table 6 verification of luminance accuracy

| | **Ground truth** | Original settings | | High noise | | Combo #1 | | Combo #2 | |
|---|---|---|---|---|---|---|---|---|---|
| **Ref Point** | luminance ($cd/m^2$) | L (cd/ $m^2$) | err (%) | L (cd/ $m^2$) | err (%) | L (cd/ $m^2$) | err (%) | L (cd/ $m^2$) | err (%) |
| **#1** | 165.5 | 167.0 | 0.9 | 160.1 | 3.3 | 164.5 | 0.6 | 168.7 | 1.9 |
| **#2** | 145.4 | 144.2 | 0.8 | 153.2 | 5.1 | 144.3 | 0.8 | 145.3 | 0.07 |
| **#3** | 208.6 | 210.1 | 0.7 | 211.5 | 1.3 | 202.2 | 3.0 | 205.5 | 1.5 |
| **#4** | 132.1 | 133.5 | 1.0 | 140.4 | 6.2 | 135.5 | 2.6 | 136.4 | 3.3 |
| **Gray** | 35.4 | 34.5 | 2.5 | 36.9 | 4.2 | 36.3 | 2.5 | 33.9 | 4.2 |

Table 6 is the luminance verification results of these four HDR images. Still, the luminance data from HDR image with the original setting shows the best results with the least error and the luminance data from HDR image with high noise settings have the lowest accuracy. The luminance accuracy from HDR image with combination setting #1 is slightly better than that with combination #2 with less standard deviation. The

luminance accuracy of HDR images with increased ISO is good with the highest error at 4.2%, which could be considered accurate in lighting research and practice. As the luminance error within 5% is considered accurate and practical mentioned in HDR photogrammetry for synchronous luminance and geometry measurement.

Table 7 verification of illuminance accuracy

| **Ground truth** | Original settings | | High noise | | Combo #1 | | Combo #2 | |
|---|---|---|---|---|---|---|---|---|
| illuminance ($lux$) | lux | Error (%) | lux | Error (%) | lux | Error (%) | lux | Error (%) |
| 337.3 | 333.3 | 1.18 | 289.5 | 14.3 | 326.9 | 3.0 | 323.1 | 4.15 |

The verification of illuminance in Table 7 shows an HDR image with the proposed strategy that partially using higher ISO value results in a smaller error rate (less than 5%) with spectrometer measured as ground truth. Maximize the film speed for taking all low dynamic range images will increase error rate to 14.3%, which is not acceptable for professional lighting measurement but fine for some tasks that only the general light level required.

Table 8 Comparison of illuminance calculation with evalglare

| | Ground truth (lux) | lux results original resolution (5184*3456) | lux results resized (1296*864) | Running speed (5184*3456) | Running speed (1296*864) |
|---|---|---|---|---|---|
| evalglare | 337.3 | 313.2 | 299.6 | 28.27 secs | 2.43 secs |
| Proposed method | | 333.3 | 327.5 | 14.10 secs | 1.86 secs |
| Proposed method (Fast) | | 323.3 | 319.2 | 4.08 secs | 1.04 secs |

Table 8 is the running speed of illuminance calculation of the proposed method and evalglare. Based on the definition of equisolid projection, a fast calculation of the proposed method is designed that all pixels can be assigned the same apparent area without calculation. Illuminance calculation of the proposed method on original pixel resolution is 2 times faster than evalglare without fast calculation and about 7 times faster with fast calculation.

## V. CONCLUSIONS

To reduce the time consumption of taking HDR images of a target scene, this study has proposed a fast speed camera-aided method with increased ISO values to take LDR images at lower exposure values. Using an improved auto-bracket program, the total time of taking 18 LDR images has been reduced from 85 seconds to less than 20 seconds. Partially using higher ISO value for taking low dynamic range images could greatly increase the capture speed with little accuracy loss (luminance error: 4.2%, illuminance: 7.6%). Maximize the ISO for taking all low dynamic range images will lift the luminance error to 6.2% and illuminance error to 14.3%, which is not acceptable for professional lighting measurement. The proposed per-pixel illuminance calculation has potential applications in human-centric tasks, and the running speed of the proposed calculation is two times faster than the illuminance calculation of evalglare and seven times faster with fast calculation. Based on the results of image noise evaluation, noise errors could be ignored for images with ISO value lower than 800, and image noise with ISO lower than 3200 is still acceptable. However, the number of LDR images with ISO 6400 should be minimized in the HDRI based lighting measurement.

## REFERENCES


[1] Alan C. Bovik (2005). Handbook of Image and Video Processing. Academic Press. ISBN 0-12-119792-1.

[2] Buades, A., B. Coll, and J.-M. Morel. "A Non-Local Algorithm for Image Denoising." 2005 IEEE® Computer Society Conference on Computer Vision and Pattern Recognition. Vol. 2, June 2005, pp. 60–65.

[3] CIE-1978. CIE Publication No. 41. Light as a true visual quantity: principles of measurement. International Commission on Illumination.

[4] Cai, H. High dynamic range photogrammetry for synchronous luminance and geometry measurement. Lighting Research & Technology, 2013 45(2): 230-257.

[5] Cai, H., Chung, T. Improving the quality of high dynamic range images. Lighting Research & Technology, 2010. 43 (1): 87-102.

[6] Erik Reinhard, Michael Stark, Peter Shirley, Jim Ferwerda, Photographic Tone Reproduction for Digital Images, SIGGRAPH 2002.

[7] Elite-cameras, 2006 "Aperture and shutter speed in digital cameras". Archived from the original on 20 June 2006.

[8] Gibson, K. D.; Scheraga, Harold A. (1987). "Exact calculation of the volume and surface area of fused hard-sphere molecules with unequal atomic radii". Molecular Physics. 62 (5): 1247–1265.

[9] Immerkær, J. "Fast Noise Variance Estimation." Computer Vision and Image Understanding. Vol. 64, Number 2, Sept. 1996, pp. 300–302.

[10] Inanici M. 2009. Introduction to high dynamic range photography. 8th International Radiance Workshop. Boston, MA.

[11] Liu, X. , Tanaka, M., Okutomi, M., 2012. Noise Level Estimation Using Weak Textured Patches of a Single Noisy Image. Proceedings of IEEE International Conference on Image Processing (ICIP2012), pp.665-668, September, 2012

[12] McCamy, Calvin S. (April 1992). Correlated color temperature as an explicit function of chromaticity coordinates".Color Research & Application. 17 (2): 142–144.

[13] Peter B. Catrysse, Xinqiao Liu, and Abbas El Gamal: QE Reduction due to Pixel Vignetting in CMOS Image Sensors; Sensors and Camera Systems for Scientific, Industrial, and Digital Photography Applications, Proceedings of SPIE, vol. 3965 (2000)

[14] Pierson C, Wienold J, Jacobs A, Bodart M. 2017b. Luminance maps from high dynamic range imaging: calibrations and adjustments for visual comfort assessment.

[15] Ray, Sidney F. 2000. "Camera Exposure Determination". In The Manual of Photography: Photographic and Digital Imaging, 9th ed. Ed. Ralph E. et al. Oxford: Focal Press. ISBN 0-240-51574-9

[16] R.M. Poling and H. Cai, 2020 .Calculatingluminousfluxradiatedtoa cameralensviahighdynamic range photogrammetry. Lighting Res. Technol. 2020; 0: 1–27

[17] S. Mann and R. W. Picard. Extending dynamic range by combining different exposed pictures. In Proc. IS&T Ann. Conf., pages 442–448, 1995. 1, 2

[18] S.Silk, J.Lang. High dynamic range image de-ghosting by fast approximate background modeling. Computer & Graphics, 2012. 1060-1071

[19] Ward, Greg, et al., 2010 'High Dynamic Range Imaging' 2nd edition, Elsevier. Burlington MA, U.S.A

[20] Wienold J, Andersen M. 2016. Evalglare 2.0 – new features faster and more robust hdr-image evaluation. Paper presented at: 15th International Radiance Workshop. Padua, Italy.